Proceedings of ASME-JSME-KSME Joint Fluids Engineering Conference 2011
AJK2011-FED
July 24-29, 2011, Hamamatsu, Shizuoka, JAPAN

AJK2011-25011

LARGE EDDY SIMULATION OF THE FLOW FIELD IN THE HUDSON RIVER

Tuy N.M. Phan
Ritsumeikan University
Kusatsu, Shiga, Japan

John C. Wells
Ritsumeikan University
Kusatsu, Shiga, Japan

William D. Kirkey
Clarkson University
Postdam, New York, USA

Mohammad S. Islam
Beacon Institute
Beacon, New York, USA

James S. Bonner
Beacon Institute
Beacon, New York, USA

ABSTRACT

Large-eddy simulation (LES) has been conducted under idealized conditions in two river reaches of the Hudson River (New York State, USA), with near-bank resolution set to some 5 meters in order to resolve large-scale motions of turbulence in the near-bank regions. To simplify analysis, simulation is performed at a constant discharge corresponding to a typical ebb tide. A standard Smagorinsky model is implemented in the commercial package FLUENT, with buoyancy neglected and bottom roughness set to zero. We perform Proper Orthogonal Decomposition (POD) on the LES results. POD modes are orthogonal flow fields that capture the kinetic energy in an optimally convergent fashion. Results show that only a few POD modes are enough to describe the most energetic flow dynamics. In a reach around the Indian Point power plant, the second and third modes reflect an interesting generation of separating eddies on the western bank, which we do not find with a URANS (standard $k\!-\!\varepsilon$) computation on the same grid. To test our simulation, a comparison of simulation results with other simulation results and Acoustic Doppler Current Profiler (ADCP) data measured at West Point, New York will be presented.

INTRODUCTION

Turbulence plays an important role in the transport of mass, momentum and heat in rivers, estuaries and oceans. Large-scale turbulent structures appearing in regions with abrupt changes in geometry such as bends, confluences strongly affect energy loss, sediment transport and pollutant spreading. The understanding and predictability of turbulence features is therefore a great need in river engineering. With the development of computer power, three-dimensional numerical simulation of river flows is becoming a feasible tool for investigating the turbulence and its influence on river dynamics as well as the fluvial environment.

Several 3D Reynolds averaged Navier-Stokes (RANS) models have been developed to simulate river flows due to its economical computational cost. Sinha et al. [1] carried out steady RANS with the standard $k\!-\!\varepsilon$ model to simulate the flow in the reach of the Columbia River. Meanwhile, Bradbrook et al. [2] and Lane et al. [3] made use of a turbulence model based on renormalization group theory (the RNG $k\!-\!\varepsilon$ model) for simulation of the confluence flow with better predictions than the standard $k\!-\!\varepsilon$ model for separated flows in confluence zones. This turbulence model also used along with the use of computational fluid dynamics software packages that offered the potential to river flow calculations [4-6]. However, the turbulence models, in which Reynolds averaged equations for mean-flow quantities are solved, only account for turbulent effects on the mean flow. Large-Eddy Simulation (LES), on the other, does not suffer from this limitation, allowing unsteady solutions that resolve turbulent structures at the scale of the computational grid. LES is usually superior to unsteady RANS (URANS) whenever large-scale structures dominate the flow and scalar transport [7]. 3D LES calculations are expensive, but with increasing computer power, there have been some attempts to apply the LES to simulate turbulent flows in natural rivers [8-10].

The Hudson River (New York State, USA) originates from Lake Tear of the Clouds, extending nearly 600 km to New York City. The Lower Hudson River, approximately 250 km long from the Federal Dam at Troy to the Battery at the southern tip of Manhattan Island, is a tidal estuary (Fig. 1a, from [11]). Depending on river discharge conditions, salinity intrusion extends from 30 to 100 km north of the Battery. The freshwater inflow above the Federal Dam ranges from 100 m^3/s in summer to the order of 2000 m^3/s in spring. Typical tidal range is 1.5 m, and the tidal velocities can reach 1 m/s during springtides [11]. This river was simulated using Estuarine, Coastal and Ocean Model (ECOM), a derivative of the Princeton Ocean Model (POM) developed by Blumberg and Mellor [12] which is based on the RANS method. The results of this simulation consisting of the velocity, temperature, salinity and water level, displayed on the New York Habor Observing and Prediction System (NYHOPS) [13], have a good agreement with measured data. However, the spatial resolution of 100 m in the horizontal and 10 points in the vertical may not suffice to capture turbulent motions in near-bank regions, especially near river bends or embayments. In this paper, we therefore apply Large Eddy Simulation for high-resolution simulation of small reaches in meanders of the Hudson River: a reach around the Acoustic Doppler Current Profiler (ADCP) measured location at West Point (Latitude 41°23'10", Longitude 73°57'20") (Fig. 1b) to test our simulation, and a second reach around the Indian Point power plant (Fig. 1c) to predict turbulent structures that are likely to trap heat in near-bank regions around the power plant.

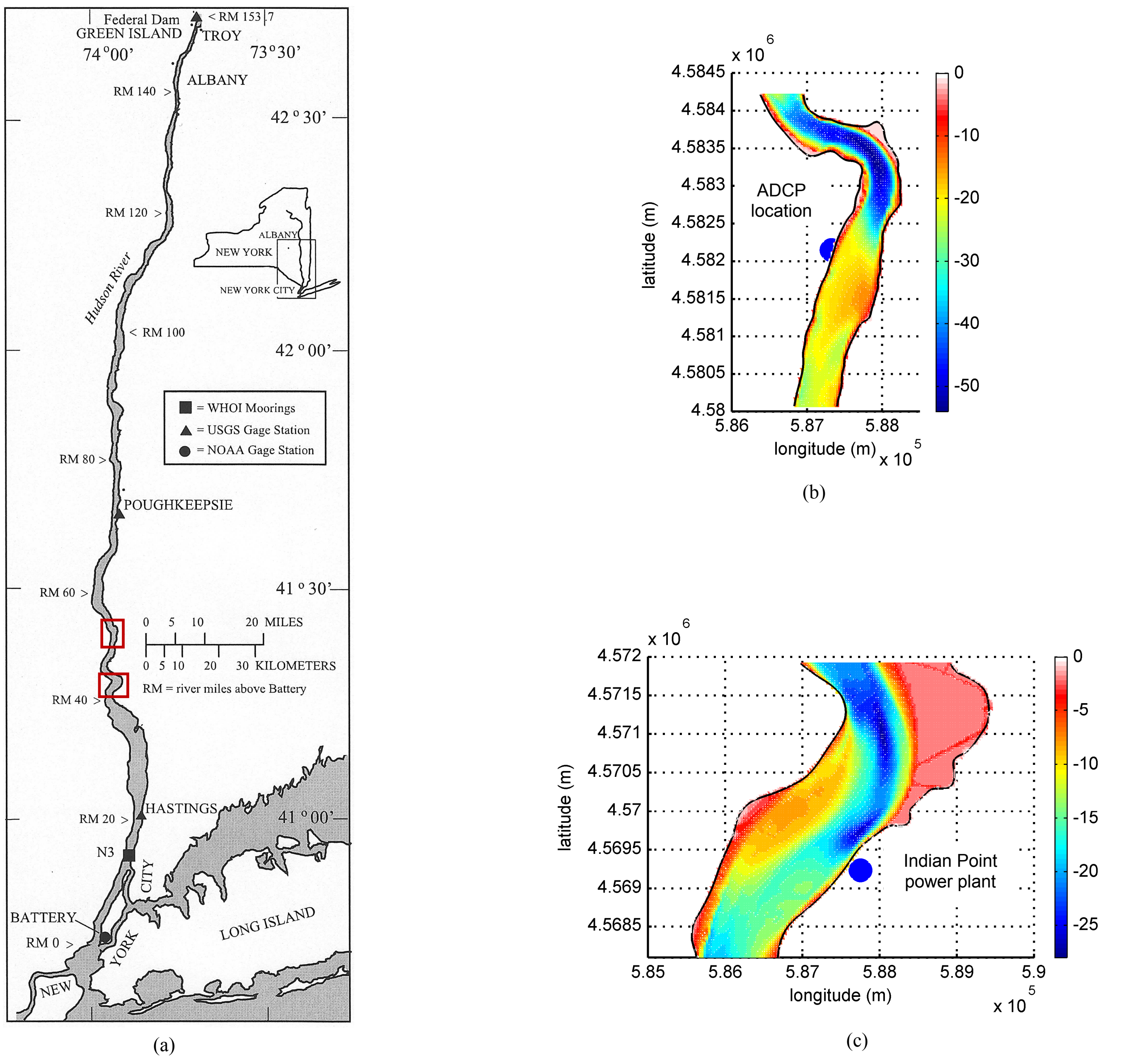

FIGURE 1. THE LOWER HUDSON RIVER (A, FROM [11]). THE LOCATION AND BED ELEVATION OF TWO REACHES: ONE AROUND ADCP MEASURED LOCATION AT WEST POINT (B) AND THE OTHER AROUND THE INDIAN POINT POWER PLANT (C).

The outline of the paper is as follows. The Large Eddy Simulation method and Proper Orthogonal Decomposition (POD), which is similar to Fourier decomposition, are first described. This is followed by a comparison of the simulation results with the NYHOPS as well as ADCP data to validate the simulation. The application of POD to the simulation results of a river reach around Indian Point power plant is then presented. Finally, we give some comments and discuss future work.

NUMERICAL MODEL

The governing equations in Large Eddy Simulation of river flows are the spatially-filtered three-dimensional incompressible continuity and Navier-Stokes equations. The filter width is determined by the grid spacing. Small-scale motions of turbulence are removed and cannot be resolved on a given grid. Instead, the effect of the unresolved turbulent motions is represented by the sub-grid-scale (SGS) stresses appearing in the filtered equations of momentum, which is modeled. The most commonly used model is based on eddy-viscosity:

$$\tau_{ij} - \frac{1}{3}\tau_{kk}\delta_{ij} = -2\mu_t \overline{S_{ij}} \tag{1}$$

where the overbar denotes the grid filtering operation and S_{ij} is the strain rate tensor. The eddy-viscosity-based model used here is the standard Smagorinsky model in which the sub-grid turbulence viscosity is modeled using a mixing-length relationship:

$$\mu_t = \rho L_s^{\,2} \left|\overline{S_{ij}}\right| \tag{2}$$

where L_s is the mixing length of sub-grid scales and $\left|\overline{S_{ij}}\right|$ is the magnitude of the strain rate tensor S_{ij}. In finite-volume method, L_s is determined by

$$L_S = \min\left(\kappa d, C_S V^{1/3}\right) \tag{3}$$

where κ is the von Karman constant, d is the distance to the closest wall, C_s is the Smagorinsky constant, and V is the volume of the computational cell.

COMPUTATIONAL SETUP

The geometry and bed topography of two study reaches of the Hudson River Estuary, a reach around Indian Point power plant and another reach around West Point, are shown in Fig. 1b and Fig. 1c. The bathymetric data [14] was obtained from Benthic Mapping Project funded by the New York State Department of Environmental Conservation (NYSDEC) in 2008, which covers the entire Hudson River Estuary. The dataset was produced from a combination of National Oceanic and Atmospheric Administration (NOAA) and SUNY Stony Brook datasets. It measures bathymetry in meters off the river's floor in the North American Vertical Datum 1988 which is referred to mean sea level. Bathymetry data is gridded by 30x30 m resolution in the North American Datum of 1983 using the Universal Transverse Mercator coordinate system. The accuracy of the data is estimated to be 1 meter in the vertical and 15 meters in the horizontal position.

For geometry modeling and mesh generation, the pre-processor Gambit® is employed. River geometries are constructed by joining points in bathymetry data to create the bed surface and projecting these faces to the water surface to create volumes. The cooper-scheme in Gambit allows for sweeping the faces meshed with quad or triangle grid at the bed through these volumes to create layers of mesh in depth. The boundary layer meshing tool is applied to the river bank to control mesh density as well as to define the spacing of mesh node rows in its vicinity.

The resolution of the grid depends on the scale of river geometry and is refined near the river bank. The horizontal grid spacing is 5 – 30 m in the study reach around Indian Point power plant with a length of approximately 5500 m, width of 1200 m, and maximum depth of 27 m. For the second reach around West Point, with a length of 5000 m, width of 500 m, and maximum depth of 54 m, the horizontal grid spacing is 2 – 20 m. At each "horizontal" grid point of two reaches, ten points are uniformly distributed in the vertical direction. As a result, the grid for the former consists of 152100 elements and, for the latter, 204180 elements.

The commercial software package Fluent is used to perform the LES of the flow field in rivers. The principle method in Fluent is a finite-volume method, converting governing equations into algebraic equations on control volumes that can be solved numerically. For low speed incompressible flows, pressure-based approach is chosen. In this method, the velocity is obtained from the momentum equations and the pressure is extracted by solving a pressure or pressure correction equation obtained by manipulating continuity and momentum equations. Coupling of the pressure and momentum equations is achieved using SIMPLE algorithm. A steady-state solution using a standard $k-\varepsilon$ turbulence model formed the initial condition for an unsteady RANS and LES simulation. The temporal integration is carried out by an implicit scheme with second-order accuracy. The spatial derivatives are approximated by the second-order central difference. The computational time step is 10 seconds for the unsteady solution.

For simplicity, we perform the simulation of Hudson River reaches corresponding to ebb tide, but at constant discharge. The constant velocity profile, given in Tab. 1, corresponding to the mean velocity in the NYHOPS image is set as the inlet boundary condition. The turbulence inflow conditions are specified by turbulence intensity of 10% and turbulence

TABLE 1. Inlet velocity boundary condition

Case	Inlet velocity (m/s)
Indian Point	0.8
West Point	0.5

viscosity ratio of 10. At the outlet, zero gradient boundary conditions are employed. The boundary condition at the bed and the bank of the river reach are the non-slip boundary condition, and the roughness effect is neglected. At the surface, time-averaged water level is given as zero compared to the mean sea level and a free-slip boundary condition is applied. Furthermore, buoyancy effects are neglected in our simulation.

PROPER ORTHOGONAL DECOMPOSITION

Lumley [15] proposed the POD as a means for defining coherent structures in turbulent flows. The POD decomposition of a velocity field $\boldsymbol{u}(\boldsymbol{x},t)$ is given by

$$\boldsymbol{u}(\boldsymbol{x},t) \cong \sum_{k=1}^{N} \zeta_k(t)\boldsymbol{\psi}_k(\boldsymbol{x}) \tag{4}$$

where $\zeta_k(t)$ are called the temporal coefficients, and $\boldsymbol{\psi}_k(\boldsymbol{x})$ are orthogonal spatial basis functions which are the eigenfunctions of the two-point auto correlation tensor $R(\boldsymbol{x},\boldsymbol{x}')$ defined as

$$R(\boldsymbol{x},\boldsymbol{x}') = \frac{1}{T}\int \boldsymbol{u}(\boldsymbol{x},t)\boldsymbol{u}(\boldsymbol{x}',t)dt \tag{5}$$

i.e. the basis functions are solutions to the Fredholm integral equation

$$\int_D R(\boldsymbol{x},\boldsymbol{x}')\cdot\boldsymbol{\psi}(\boldsymbol{x}')d\boldsymbol{x}' = \lambda\boldsymbol{\psi}(\boldsymbol{x}) \tag{6}$$

Thus, it may be shown that they are statistically optimal in that their energy converges faster than any other set of functions in Hilbert space [16]. The eigenvalues λ represent the kinetic energy of the flow in each POD mode. Since the POD decomposition is a spectral decomposition or an eigendecomposition in which the eigenfunctions and eigenvalues are sorted in order of decreasing eigenvalue, the eigenvalues in the lower order modes are always larger than the higher order modes.

The decomposition also satisfy the orthogonal property

$$\int_D \boldsymbol{\psi}_i(\boldsymbol{x})\cdot\boldsymbol{\psi}_j(\boldsymbol{x})d\boldsymbol{x} = \delta_{ij} \tag{7}$$

$$\frac{1}{T}\int_0^T \zeta_i(t)\zeta_j(t)dt = \lambda_i\delta_{ij} \tag{8}$$

RESULTS AND DISCUSSION

Time-averaged surface velocity field in large-eddy simulation of the Hudson River around the ADCP measured location at West Point was compared with a snapshot referred from the website of the NYHOPS [13] at 23:00 November 15th, 2010 as shown in Fig. 2. The NYHOPS snapshot was chosen in condition that the inlet velocity could match as well as possible with the inlet boundary condition in our simulation. At that time, the wind velocity was about 1 m/s and the bottom salinity was nearly zero, i.e. these effects may be neglected. The result shows the simulation and the NYHOPS are in good agreement, except in near-bank regions due to the difference in the shape of the bank. Moreover, it should be noted that the simulation in the NYHOPS made used of a URANS method which is often unable to capture well dominant structures in near-bank regions with an abrupt change in geometry.

Figure 3 shows time series of ADCP velocity data from 12:00 November 15th, 2010 to 12:00 November 16th, 2010 at three horizontal distances d from the location of ADCP sensor. Vectors represent flow direction in time. The ADCP is installed horizontally on pier near the USGS gauging station at West Point on the western bank of the Hudson River. It measures the velocity on a horizontal transect of the river at the approximate depth of 3 – 4 m from the river bed with the resolution in time of 1 minute. We take the ADCP data at the same time of the above NYHOPS snapshot to compare with our simulation. At that time, as can be seen from Fig. 3, the direction of the flow at d = 2 m is different with that at d = 10 m and 80 m. This may be because of the generation of near-bank vortices upstream of the location of the ADCP.

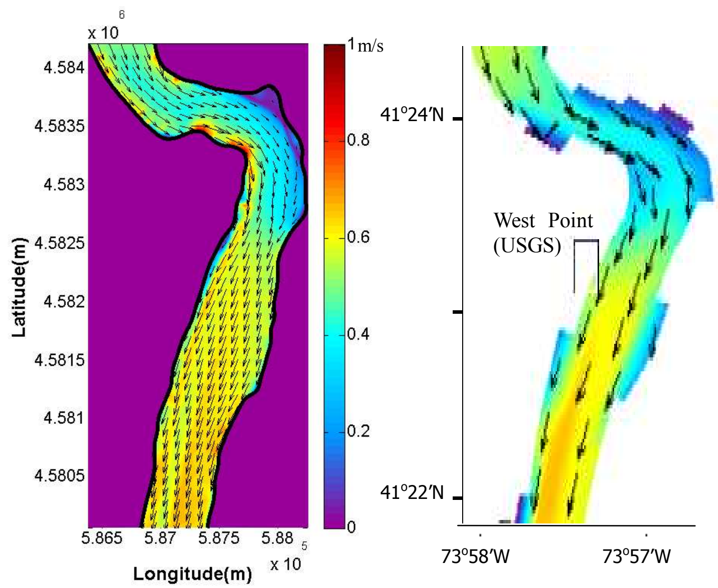

(a) (b)

FIGURE 2. COMPARISON OF TIME-AVERAGED SURFACE VELOCITY FIELD OF LES SIMULATION (A) AND A SNAPSHOT ON THE NYHOPS SYSTEM AT 23:00, NOV 15th, 2010 (B) IN THE HUDSON RIVER AROUND WEST POINT, NY (USGS). COLOR IS VELOCITY MAGNITUDE.

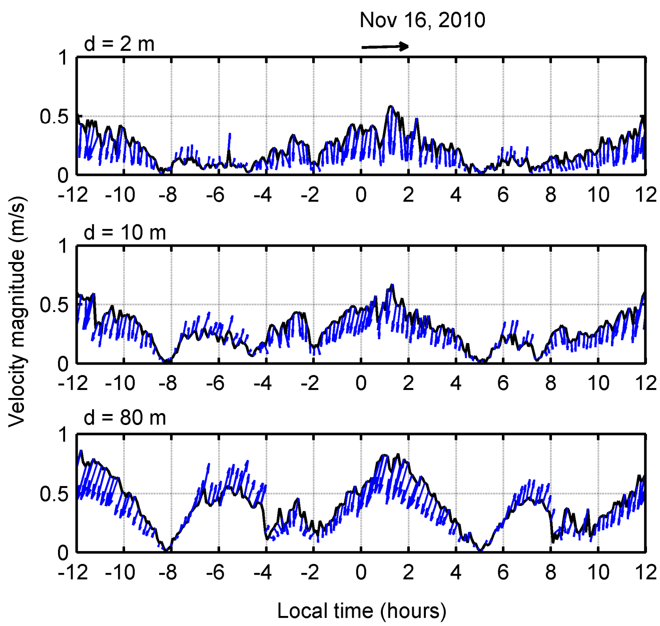

FIGURE 3. TIME SERIES OF ADCP VELOCITY DATA AT HORIZONTAL DISTANCES *D* = 2, 10 AND 80 M FROM THE LOCATION OF ADCP SENSOR AT WEST POINT. VECTORS SHOW FLOW DIRECTION.

Figure 4 shows a comparison of time-averaged velocity in our simulation, URANS (standard k–ε) and LES, with a series of ADCP data from 22:55 to 23:05, November 15th, 2010 at four different horizontal distances *d* from the ADCP sensor. Results show that URANS and LES give velocity larger than the measured data. It may be because that there is a difference in discharge between simulation and ADCP measurement. Besides, in the near-bank regions, time-averaged velocities of LES are found to be clearly different compared with those of URANS. The occurrence of turbulent structures near the bank might explain these findings. Farther from the river bank, velocities in LES and URANS are similar, with the magnitude of 0.63 m/s. Meanwhile, velocity measured by ADCP is 0.41 m/s, smaller than those in our simulation. For reference, the surface velocity simulated in the NYHOPS at that time is 0.56 m/s at West Point USGS gauging station.

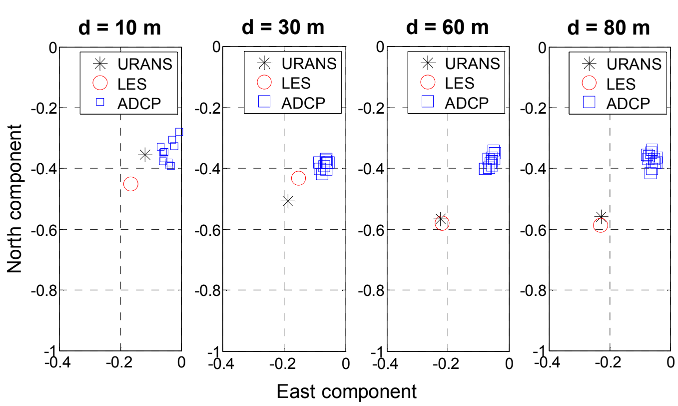

FIGURE 4. COMPARISON OF TIME-AVERAGED VELOCITY IN URANS - STANDARD K-EPSILON MODEL (STAR SYMBOL), LARGE EDDY SIMULATION (CIRCLE SYMBOL) AND A TIME SERIES OF ADCP (SQUARE SYMBOL) FROM 22:55 TO 23:05, NOV 15, 2010 AT HORIZONTAL DISTANCES *D* = 10 M, 30 M, 60 M AND 80 M.

Figure 5, 6 and 7 show results of the surface velocity POD decomposition from 300 LES snapshots of the Hudson River around Indian Point power plant. Time interval between 2

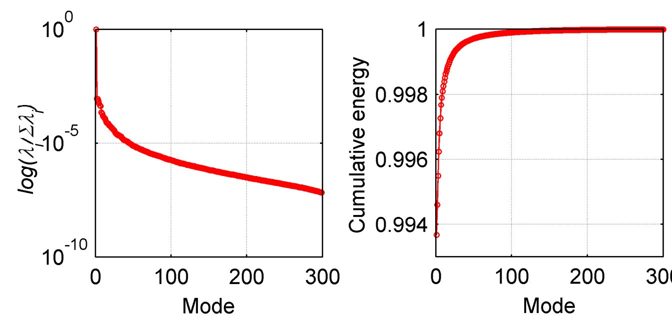

FIGURE 5. REACH AROUND INDIAN POINT: ENERGY SPECTRUM AND CUMULATIVE ENERGY OF POD VELOCITY DECOMPOSITION FROM 300 LES SNAPSHOTS OF SURFACE VELOCITY. TIME INTERVAL BETWEEN 2 SNAPSHOTS IS 650 S.

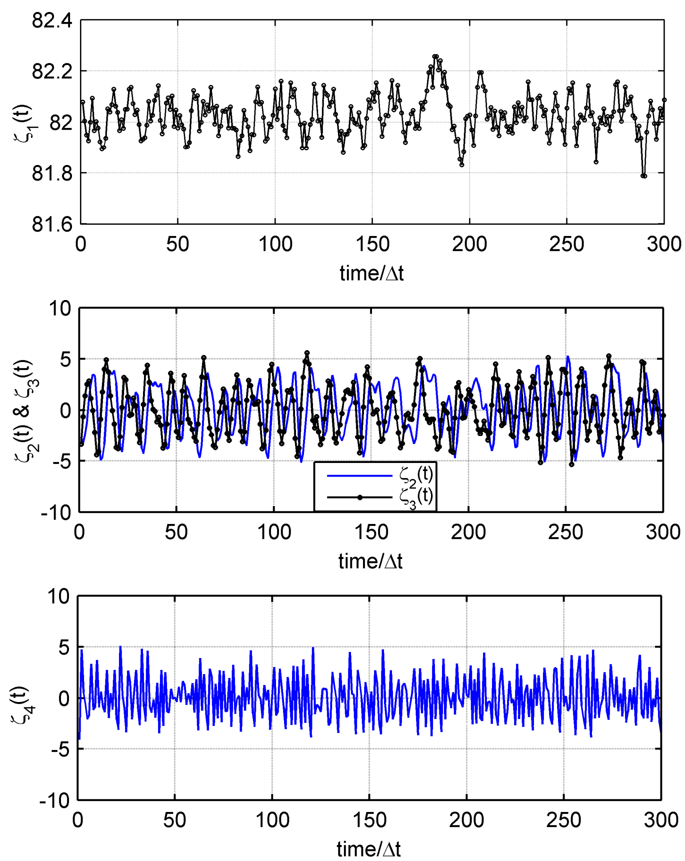

FIGURE 6. POD COEFFICIENTS. SOLID LINES ARE EVEN COEFFICIENTS.

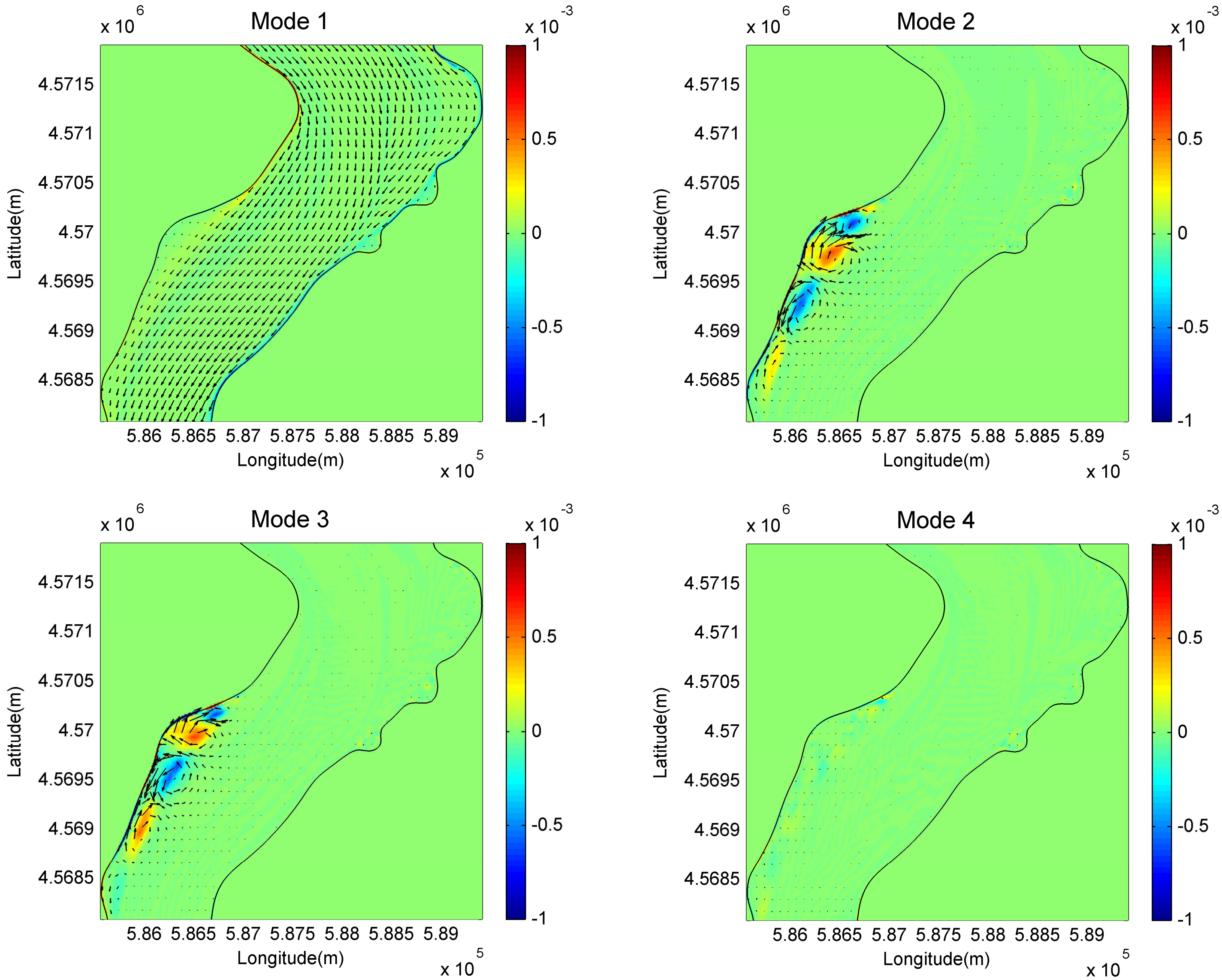

FIGURE 7. LOW-ORDER POD VELOCITY MODES. COLOR IS CORRESPODING VORTICITY OF POD MODES

snapshots is 650 s. The energy spectrum and cumulative energy of the 300 POD modes are shown in Fig. 5. The eigenvalues are equivalent to the amount of energy that is captured in each mode, and the sum of the eigenvalues equals the total energy. Energy contained in mode 1 is found to contribute nearly 99.4% of the total energy of the flow. The time evolution of the POD coefficients of mode 1 – 4 is shown in Fig. 6. The first 4 POD basis functions and their corresponding vorticity are shown in Fig. 7. The POD coefficient in higher modes is found to fluctuate at more rapidly. Mode 1 has the highest POD coefficient and its POD basis function should be equivalent to the mean flow. The POD basis functions in mode 2 and 3 define an interesting generation of vortices on the western bank due to the shear layer in shallower region. It can be found that the vortices in these two modes as wells as their corresponding POD coefficients phase difference of nearly 90^{o} in time. These low-order modes shown in Fig. 7 can reveal statistically dominant structures, which capture most of the energy of the flow (99.6%). If the flow in rivers or oceans is found to be low-dimensional, only a few modes can reproduce the essential dynamics. In order to exploit the efficiency of such low-dimensional representations, both the data assimilation problem and the forecasting problem can be re-formulated using the POD modes.

CONCLUSION

In this paper, large eddy simulation of two small reaches of the Hudson River, a river reach around the Indian Point power plant and the other around the West Point ADCP measured location, has been done in Fluent, a CFD software based on finite volume method. We concentrate on simulating the flow field at a constant discharge corresponding to a typical ebb tide. The standard Smagorinsky model is used with assumption of no buoyancy and zero wall roughness.

To test our simulation, the LES simulation is compared with NYHOPS and ADCP data at West Point at the same time. Results show that the simulation gives the velocity larger than ADCP data. Meanwhile, the simulation looks good agreement with the NYHOPS.

We also perform Proper Orthogonal Decomposition from 300 LES snapshots of the river reach around the Indian Point power plant. The POD results show that only a few low-order POD modes capture the large energy content of the flow. Therefore, these modes can be used to describe dynamics in complex, multi-scale flow in rivers, estuaries and oceans. We hope that real-time prediction of 3D turbulent flow field can be done by tracking the evolution of POD coefficients for a long time using Kalman filter.

In the future work, we will extend our simulation to full typical tidal cycles. Wall roughness will be applied to the simulation based on bed surface material of the study reach. Besides, thermal impact of Indian Point power plant will be studied.

ACKNOWLEDGEMENT

The first author is grateful for a scholarship from the Japanese government (MEXT) during her study.

REFERENCES

[1] Sinha S. K., Sotiropoulos F., and Odgaard A. J., 1998. "Three-dimensional numerical model for flow through natural rivers". *Journal of Hydraulic Engineering*, **124**(1), pp. 13–24.

[2] Bradbrook K. F., Biron P. M., Lane S. N., Richards K. S., and Roy A. G., 1998. "Investigation of controls on secondary circulation in a simple confluence geometry using a three-dimensional numerical model". *Hydrol. Process.*, **12**(8), pp. 1371-1396.

[3] Lane S. N., Bradbrook K. F., Richards K. S., Biron P. A., and Roy A. G., 1999. "The application of computational fluid dynamics to natural river channels: three-dimensional versus two-dimensional approaches". *Geomorphology*, **29**(1-2), pp. 1-20.

[4] Hodskinson A., and Ferguson R. I., 1998. "Numerical modelling of separated flow in river bends: model testing and experimental investigation of geometric controls on the extent of flow separation at the concave bank". *Hydrol. Process.*, **12**(8), pp. 1323-1338.

[5] Ma L., Ashworth P. J., Best J. L., Elliott L., Ingham D. B., and Whitcombe L. J., 2002. "Computational fluid dynamics and the physical modelling of an upland urban river". *Geomorphology*, **44**(3-4), pp. 375-391.

[6] Rodriguez J. F., Bombardelli F. A., García M. H., Frothingham K. M., Rhoads B. L., and Abad J. D., 2004. "High-resolution numerical simulation of flow through a highly sinuous river reach". *Water Resources Management*, **18**(3), pp. 177-199.

[7] Rodi W., 2010. "Large eddy simulation of river flows". In Proceedings of the International Conference on Fluvial Hydraulics, Bundesanstalt fur Wasserbau, Karlsruhe, Germany, pp. 23-32.

[8] Bradbrook K. F., Lane S. N., Richards K. S., Biron P. M., and Roy A. G., 2000. "Large Eddy Simulation of periodic flow characteristics at river channel confluences". *Journal of Hydraulic Research*, **38**(3), p. 207.

[9] Kang S., Lightbody A., Hill C., and Sotiropoulos F., 2011. "High-resolution numerical simulation of turbulence in natural waterways". *Advances in Water Resources*, **34**(1), pp. 98-113.

[10] Stoesser T., Ruether N., and Olsen N. R. B., 2010. "Calculation of primary and secondary flow and boundary shear stresses in a meandering channel". *Advances in Water Resources*, **33**(2), pp. 158-170.

[11] Warner J. C., Geyer W. R., and Lerczak J. A., 2005. "Numerical modeling of an estuary: A comprehensive skill assessment". *J. Geophys. Res.*, **110**, p. 13 PP.

[12] Blumberg A. F., and Mellor G. L., 1987. "A description of a three-dimensional coastal ocean circulation model". *Three-dimensional coastal ocean models*, **4**, pp. 1–16.

[13] URL http://hudson.dl.stevens-tech.edu/maritimeforecast/maincontrol.shtml

[14] URL http://www.nysgis.state.ny.us/gisdata/inventories/details.cfm?DSID=1136.

[15] Lumley J. L., 1967. "The structure of inhomogeneous turbulent flows" In Atmospheric turbulence and radio wave propagation, A. M. Yaglom and V. I. Tatarsky, eds., Nauka, pp. 166–178.

[16] Holmes P., Lumley J. L., and Berkooz G., 1996. *Turbulence, coherent structures, dynamical systems and symmetry.* Cambridge University Press, Cambridge.